

# Interactions between Lead–Zirconate Titanate, Polyacrylic Acid, and Polyvinyl Butyral in Ethanol and Their Influence on Electrophoretic Deposition Behavior

Danjela Kuscer\*

Jožef Stefan Institute, Jamova 39, SI-1000 Ljubljana, Slovenia  
Centre of Excellence NAMASTE, Jamova 39, SI-1000 Ljubljana, Slovenia

Tina Bakarič\*

Jožef Stefan Institute, Jamova 39, SI-1000 Ljubljana, Slovenia

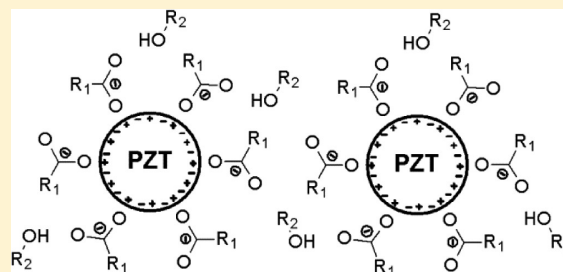
Bojan Kozlevčar\*

Faculty of Chemistry and Chemical Technology, University of Ljubljana, Aškerčeva c. 5, SI-1000 Ljubljana, Slovenia

Marija Kosec\*

Jožef Stefan Institute, Jamova 39, SI-1000 Ljubljana, Slovenia  
Centre of Excellence NAMASTE, Jamova 39, SI-1000 Ljubljana, Slovenia

**ABSTRACT:** Electrophoretic deposition (EPD) is an attractive method for the fabrication of a few tens of micrometer-thick piezoelectric layers on complex-shape substrates that are used for manufacturing high-frequency transducers. Niobium-doped lead–zirconate titanate (PZT Nb) particles were stabilized in ethanol using poly(acrylic acid) (PAA). With Fourier-transform infrared spectroscopy (FT-IR), we found that the deprotonated carboxylic group from the PAA is coordinated with the metal in the perovskite PZT Nb structure, resulting in a stable ethanol-based suspension. The hydroxyl group from the polyvinyl butyral added into the suspension



to prevent the formation of cracks in the as-deposited layer did not interact with the PAA-covered PZT Nb particles. PVB acts as a free polymer in ethanol-based suspensions. The electrophoretic deposition of micro- and nanometer-sized PZT Nb particles from ethanol-based suspensions onto electroded alumina substrates was attempted in order to obtain uniform, crack-free deposits. The interactions between the PZT Nb particles, the PAA, and the PVB in ethanol will be discussed and related to the properties of the suspensions, the deposition yield and the morphology of the as-deposited PZT Nb thick film.

## INTRODUCTION

Piezoelectric thick-films based on lead–zirconate titanate with a tailored thickness and porosity have been widely used for the fabrication of high-frequency ultrasound transducers that enable a noninvasive visualization of living tissue with a resolution of the order of 50  $\mu\text{m}$ .<sup>1–3</sup> High-frequency transducers operating at 40–60 MHz for ocular, skin, or intravascular imaging consist of a 20–30  $\mu\text{m}$  thick piezoelectric with a porosity of around 25 vol %.<sup>2</sup> To improve the device's sensitivity and its resolution, the piezoelectric layer is patterned on a nonflat mechanical support, acting as a backing.<sup>4</sup> Electrophoretic deposition (EPD) has been considered as an effective technique for the processing of thick films on complex-shape substrates.<sup>5,6</sup> Additionally, EPD provides

considerable control over the thickness of the as-deposited layer and over the deposition rate, and with a subsequent sintering process, EPD enables the formation of homogeneous thick films with a tailored thickness and porosity.

When conducting EPD, the particles must be electrically charged to create deposits on the oppositely charged electrode. Anionic polyelectrolytes, such as a poly(acrylic acid) (PAA), are widely used as the dispersants of ceramic powder in aqueous media. The repulsive forces between the particles and,

**Special Issue:** Electrophoretic Deposition

**Received:** May 31, 2012

**Revised:** September 28, 2012

**Published:** October 1, 2012

accordingly, the stability of the dispersion depend on the polyelectrolyte adsorption on the particle. This is regulated by the chemical composition and the molar mass of the polyelectrolyte, the nature of the particle surface, and the dispersion properties. The degree of dissociation and the conformation of the PAA strongly depend on the pH of the dispersion. At a low pH, around a pH 3, the PAA is not dissociated and is in the coil conformation; above a pH of 10, the PAA is dissociated and is in an extended tail configuration.<sup>7–10</sup> The PAA is not soluble in ethanol. However, it was demonstrated that the poly methacrylic acid (PMAA) and PAA can effectively stabilize alumina, zirconia, and PZT particles in ethanol in the presence of *n*-butylamine.<sup>4,11,12</sup> Additionally, the properties of the EPD deposits from alumina and zirconia dispersions depend strongly on the concentration and the addition sequence of the two additives.<sup>11,12</sup>

Polyvinyl butyral (PVB) is frequently used as an additive in ceramic processing. It acts as a binder that provides green strength for handling and may also inhibit crack formation. PVB interacts with metal-oxide particles and therefore may impact the stability of the ceramic suspension as well as the deposition process during EPD.<sup>13–15</sup> PVB contains a hydroxyl group via polyvinyl alcohol (PVA) that dominates the adsorption of PVB on yttria-stabilized zirconia (YSZ) particles by hydrogen bonding.<sup>15</sup> A large number of hydroxyl groups leads to a more adsorbed amount of PVB on the particles and the lower mobility of YSZ particles in the toluene–ethanol solvent. The resulting green deposit obtained by EPD was thicker, but more porous, than the deposit from the suspension containing PVB with a smaller number of hydroxyl groups.<sup>15</sup> When the particles are already stabilized by the anionic polyelectrolyte, the coadsorption of polyvinyl alcohol is not favorable at basic medium.<sup>14</sup>

The drying of the as-deposited layer is a critical step in the processing of thick-film structures. It was reported that, above a critical thickness of as-deposited layer, it cracks spontaneously, regardless of the drying rate. The critical thickness of the layer depends, among other things, on the morphology of the powder, its particle size, and the packing.<sup>16</sup> Suspensions containing well-dispersed, uniform, nanosized particles are particularly useful for improving the packing density of the as-deposited layers.<sup>17</sup> The sintering of thick films on a substrate is another critical step. At elevated temperatures, the film tends to shrink due to the driving force for sintering, but it is clamped to the rigid substrate. The stress developing in the film due to the constraint is relaxed via the formation of processing defects such as the formation of cracks or the growth of pores in the films.<sup>18</sup> In addition, the diffusion processes and lead-loss in lead-based materials are significant at elevated temperatures, and therefore, the lowering of the processing temperature is an important approach.<sup>19</sup>

Numerous researchers have studied the processing of PZT thick films by EPD. After sintering, the layer thicknesses between 5 and 20  $\mu\text{m}$  are reported from a one-step deposition process.<sup>20–22</sup> It seems that the formation of cracks in layers with a thickness of a few tens of micrometers during the processing is a problem. Therefore, the reported thicknesses appear to be the limiting thickness for sintered PZT films.

In this article, we present an experimental investigation that is focused on the electrophoretic deposition of niobium-doped lead-zirconate titanate (PZT Nb) particles from ethanol-based suspensions. We consider in detail the interactions between PZT Nb particles and poly(acrylic acid) in ethanol during the

process of milling. The role of the polyvinyl butyral on the dispersion of the PZT Nb/PAA particles in ethanol and its influence on the deposition process and morphology of the deposits were investigated.

## ■ EXPERIMENTAL METHODS

Pb( $\text{Zr}_{0.53}\text{Ti}_{0.47}$ )<sub>0.98</sub>Nb<sub>0.02</sub>O<sub>3</sub> (denoted PZT Nb) powders were synthesized from PbO (99.9%, Aldrich, Germany), ZrO<sub>2</sub> (99.1%, Tosoh, Japan), TiO<sub>2</sub> (99.8%, Alfa Aesar, Germany), and Nb<sub>2</sub>O<sub>5</sub> (Sigma Aldrich, 99.9%) by solid-state synthesis. The oxides were homogenized in a planetary mill for 2 h. After drying, the mixture was calcined at 1100 °C for 2 h, remilled, and recalcined. After a second calcination, the powder was milled for 6 h in an attritor mill and dried.

The electrophoretic deposition experiments were performed using ethanol-based suspensions containing 1 vol % of PZT Nb powder that were prepared as follows. Polyacrylic acid (PAA) from Alfa Aesar (50 wt % of PAA in water; molar mass 2000) was mixed with *n*-butylamine (BA) from Alfa Aesar. The amount of PAA is given as a mol of PAA per mass of PZT Nb powder, i.e.,  $\mu\text{mol/g}$ . The PAA/BA molar ratio was varied from 1/2.5 to 1/10. At a fixed PAA/BA ratio of 1/2.5, the amount of PAA was varied from 50 to 150  $\mu\text{mol/g}$ . Into the PAA and BA mixture, we added ethanol (Carlo Erba). These solutions were used for the optimization of the PAA/BA ratio. The PZT Nb powder was added to the solutions. The suspension was mixed with a magnetic stirrer at 150 rpm for 30 min, followed by homogenization of the suspension in a ZrO<sub>2</sub> planetary mill at 150 rpm for 1 h. Selected suspensions were additionally milled in a colloidal mill (MiniCer, NETZSCH, Hann, Germany) at 1500 rpm up to 3 h. YSZ balls with a diameter of 0.3 mm were used as the grinding medium. The suspension-to-balls volume ratio was 1:1. The total suspension volume was 250 mL.

In some cases, polyvinyl butyral (PVB, Aldrich, molar mass 50 000–80 000) was added to the suspension. A total of 1 and 3 wt % of PVB was added to the PZT Nb ethanol-based suspension and mixed with a magnetic stirrer for 8 h.

A standard electrophoretic deposition setup was employed. The vertically aligned electrodes were separated by a distance of 17 mm. Two identical Al<sub>2</sub>O<sub>3</sub> square-plates (Kyocera, 99.9%) with a thickness of 0.5 mm and a length of 12.5 mm, covered on one side by gold electrodes (ESL 8884-G), were used as the working and counter electrodes. The area of the electrode was 0.64 cm<sup>2</sup>. The deposition process was performed at a constant current density of 1.56 mA/cm<sup>2</sup>, provided by a Keithley 2400 source meter. The experiments were conducted at ambient temperature and without any mechanical stirring. The deposition times varied between 15 and 150 s. After the deposition, the samples were placed in an ethanol-rich atmosphere and dried at ambient temperature.

The particle size and the particle-size distribution were determined using a static light-scattering particle-size analyzer (Microtrac S3500, USA). All the presented results were derived from the volume particle size distributions, denoted as  $d_v$ . The specific surface area of PZT Nb powder was analyzed using the N<sub>2</sub> adsorption BET method (NOVA 2200E, Quantachrome Instruments, Boynton Beach, USA). The powder was dried at 50 °C and subsequently degassed at 200 °C for 2 h prior to the measurement. The morphologies of the deposits was investigated with a scanning electron microscope (SEM) (JEOL 7600, Tokyo, Japan). The zeta potential of the particles was measured in diluted ethanol dispersions using a zeta potential analyzer ZetaPALS (Brookhaven Instruments Corpo-

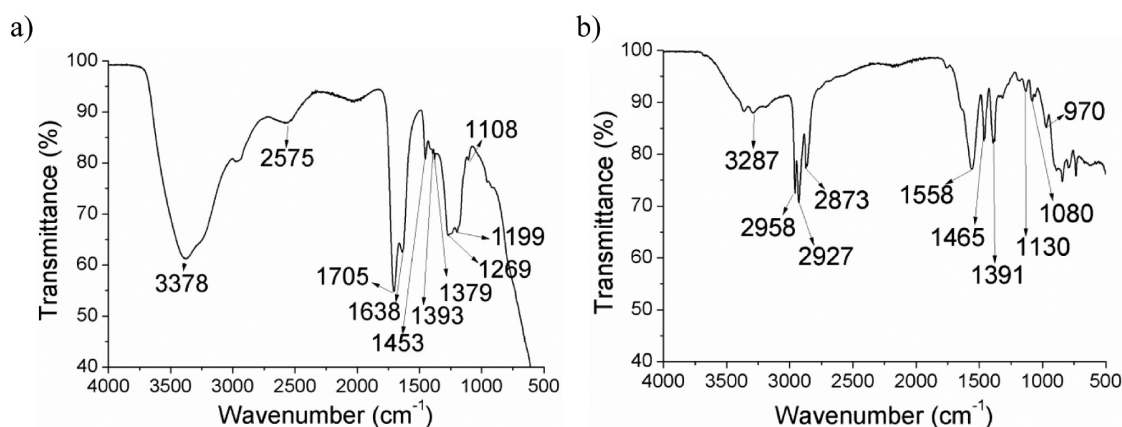


**Figure 1.** FT-IR spectra of (a) PAA–water solution at pH 3 and (b) solution of PAA and BA with PAA/BA ratio 1:2.5.

ration, USA). The viscosity of the suspensions was determined at 25 °C at shear rates between 10 and 100 s<sup>−1</sup> after an equilibration period of 30 s with a CC 27 cylindrical system using a Physica MCR 301 rheometer (Anton Paar, Austria). The FT-IR spectra of the PZT Nb powder were obtained from powders dried at 50 °C using a Perkin-Elmer 100 Fourier Transform Infrared Spectrometer. The PZT Nb powder was separated from the suspensions, washed, and dried at 50 °C. The FT-IR spectra of the samples were recorded in the range 4000–400 cm<sup>−1</sup>. The FT-IR spectra of as-received PAA water solution, the PAA–BA solution, and the PVB powder were also collected.

## RESULTS AND DISCUSSION

When dispersing micrometer-sized PZT Nb particles in ethanol without any additives, the suspensions were observed to become unstable. The sediment, accompanied by a clear supernatant, was observed after less than a minute. The positive zeta potential of +20 mV indicated the formation of positively charged PZT Nb particles as a result of the adsorption of alcohol at the particle surfaces.<sup>23</sup> In order to improve the suspension stability, the PAA as a charging additive was investigated.

The PAA was dissolved in ethanol in the presence of BA.<sup>12</sup> The minimal PAA/BA molar ratio that allows the formation of a clear solution is 1:2.5. For smaller amounts of BA, the PAA–BA–ethanol solution contained a solid phase that did not dissolve in ethanol, despite stirring the solution for more than 12 h. We believe that, for a small amount of BA, the solution has an acidic character that does not favor the dissociation of PAA.

The as-received PAA water solution with pH 3 consisted of nondissociated COOH groups, as is evident from the FT-IR spectrum (Figure 1a). The band at 1705 cm<sup>−1</sup> is assigned to the C=O double bond, while 1269 and 1199 cm<sup>−1</sup> bands are assigned to the C–O single-bond vibration characteristic for carboxylic acid COOH groups. In the FT-IR spectrum of the solution with a PAA/BA ratio of 1:2.5 (Figure 1b), the bands at 1558 and 1391 cm<sup>−1</sup> are assigned to the asymmetrical and symmetrical stretching vibrations of the anionic carboxylate group.<sup>24</sup> These bands and the absence of the 1700 and 1200 cm<sup>−1</sup> bands (evidenced in the as-received PAA) are a clear indication of a deprotonation, resulting in a final anionic PAA.

In order to optimize the PAA/BA ratio, we measured the conductivity of the ethanol-based solutions containing 0.020 mol/L PAA and various amounts of BA corresponding to a

PAA/BA ratio between 1:2.5 and 1:10. The conductivity of the solutions increased with an increasing amount of BA, and therefore, a low PAA/BA ratio is favored for the EPD (Figure 2). Following these results, further experiments were carried out at constant PAA/BA ratio of 1:2.5.

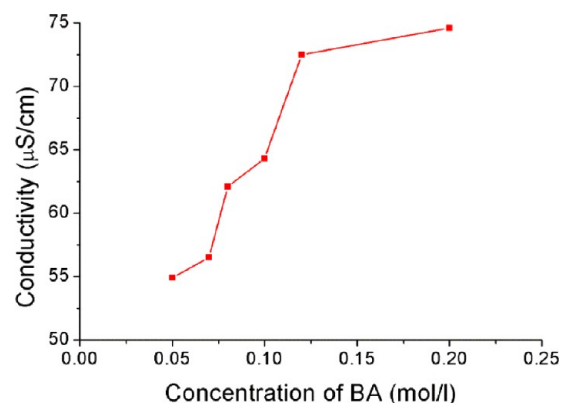


**Figure 2.** Conductivity of PAA and BA ethanol solution containing 0.02 mol PAA/L as a function of the amount of BA.

Our first series of experiments on ethanol-based PZT Nb suspensions consisted of the optimization of the amount of PAA at the optimal PAA/BA ratio for micrometer-sized PZT Nb particles. The conductivity of a 1 vol % PZT Nb suspension in ethanol and the zeta potential of the PZT Nb particles in ethanol with various amounts of PAA at a PAA/BA ratio of 1:2.5 are presented in Figure 3. With the increasing amount of PAA, the absolute value of the zeta potential increases from −38 to −59 mV at 50 and 125 μmol PAA/g. Simultaneously, the conductivity of the suspension increases. A low conductivity and a high absolute value of the zeta potential are favorable for EPD. In response to these results, it is difficult to identify the optimal parameters of the suspension suitable for EPD since both the conductivity and the zeta potential play a significant role in the deposition process.

We investigated the PZT Nb yield from an ethanol-based dispersion as a function of the amount of PAA and of the deposition time at a constant PAA/BA ratio of 1:2.5. From the Figure 4, it is evident that the mass of the deposit decreases with the increasing amount of PAA up to 100 μmol/g for a deposition time of 120 s at a constant current density of 1.56 mA/cm<sup>2</sup>. With the further addition of PAA, the mass of the deposit did not vary significantly and is, within the experimental



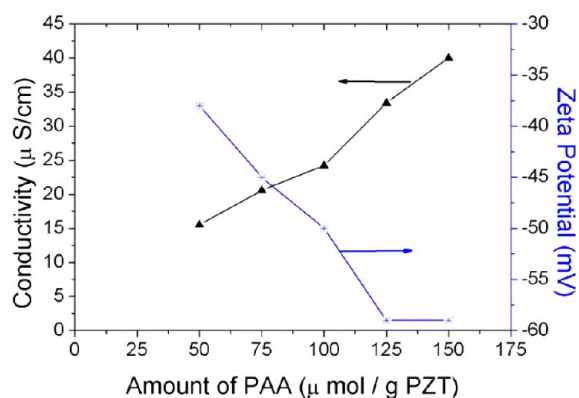


**Figure 3.** Conductivity of 1 vol % PZT Nb ethanol-based suspension and zeta potential of PZT Nb particles as a function of PAA amount at a PAA/BA ratio of 1:2.5.

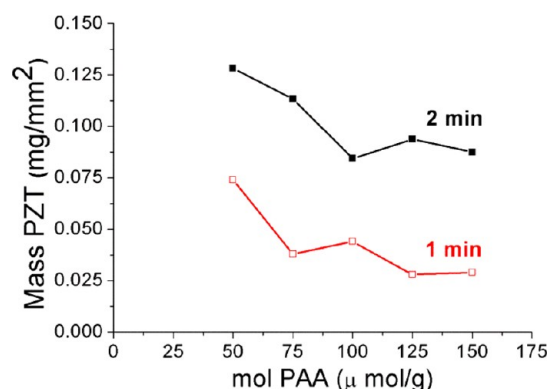


**Figure 4.** Yield of PZT Nb from 1 vol % PZT Nb ethanol-based suspensions as a function of PAA amount and deposition time at a PAA/BA ratio of 1:2.5.

uncertainty, almost constant. Similar behavior was observed for the deposition time of 60 s.

The surface morphology of the dried thick-films deposited at a constant current density of  $1.56 \text{ mA/cm}^2$  for 120 s containing 50, 100, and  $150 \mu\text{mol PAA/g}$  was investigated by SEM. Typical images of the deposits are shown in Figure 5a–c. From these images, it is evident that the morphology of the deposits is different. The most uniform deposit was obtained from the suspension containing  $100 \mu\text{mol PAA/g}$ . This deposit was smooth and consisted of uniformly distributed, micrometer-sized PZT Nb particles (Figure 5b). The deposit from the suspension containing  $50 \mu\text{mol PAA/g}$  contained uniform regions separated by a group of pores (Figure 5a). The surface of the deposit from the suspension containing  $150 \mu\text{mol PAA/g}$  (Figure 5c) was the roughest and consisted of a larger number of pores. From the SEM images, we found that the most uniformly deposited layers were produced from the suspension containing  $100 \mu\text{mol PAA/g}$ . Since the deposits were prepared from the same PZT Nb powder at identical deposition and drying conditions, their dissimilar morphology should originate from the polymer–particle interactions in the solvent. When the amount of PAA in the suspension increased, the conductivity of the suspension and the absolute value of the zeta potential on the particles increased. The conductivity of the suspensions increases from 15 to 24 and  $40 \mu\text{S/cm}$  for 50, 100, and  $150 \mu\text{mol PAA/g}$ , respectively. The absolute value of the zeta potential on the PZT Nb particles increases from  $-38$  to  $-50$  and  $-59 \text{ mV}$  for 50, 100, and  $150 \mu\text{mol PAA/g}$ ,

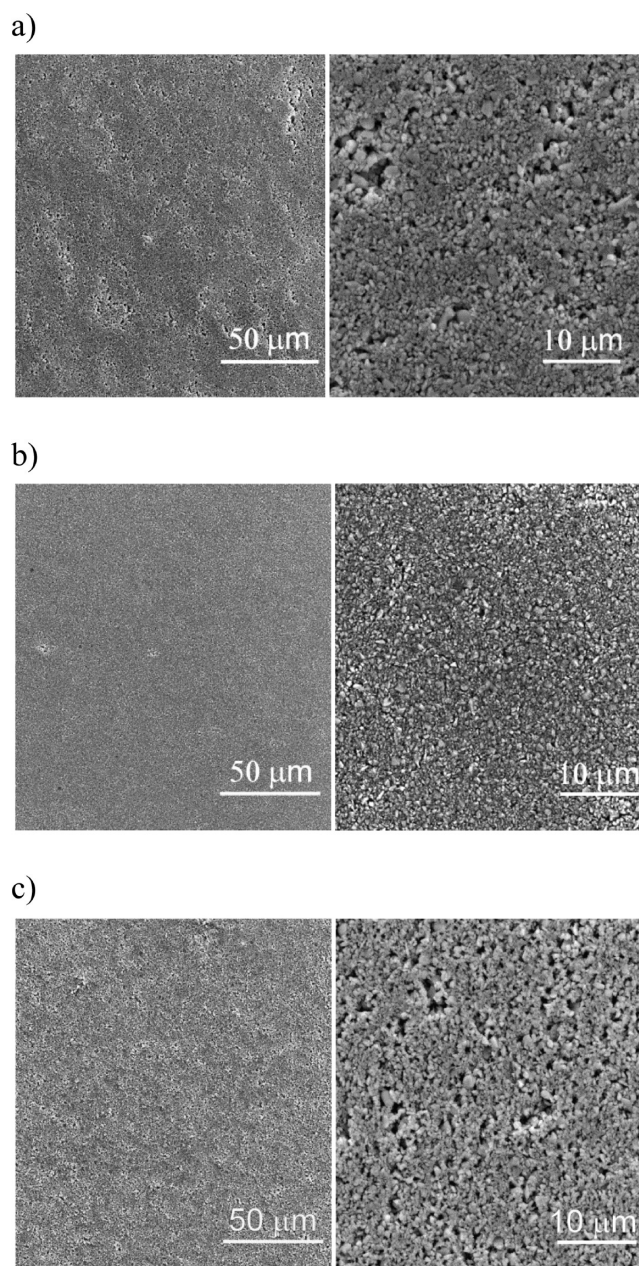


**Figure 5.** Electron microscopy surface image of as-deposited PZT Nb thick-films from ethanol suspensions containing 1 vol % PZT Nb and a PAA/BA ratio of 1:2.5. EPD was performed at constant current density of  $1.56 \text{ mA/cm}^2$  for 120 s. The amount of PAA was (a) 50, (b) 100, and (c)  $150 \mu\text{mol/g}$ .

respectively. Stappers et al.<sup>25</sup> showed that the electrolyte's conductivity had an effect on the uniformity of the deposit. Nonuniform deposits were obtained from alumina–ethanol suspensions with a low conductivity of  $3.2$  and  $7.8 \mu\text{S/cm}$ . The uniformity of the deposit was improved when high-conductivity suspensions were used, i.e.,  $38$  and  $67 \mu\text{S/cm}$ . In our case, for a  $50 \mu\text{mol PAA/g}$  suspension, its conductivity is relatively low, i.e.,  $15 \mu\text{S/cm}$ , and the zeta potential of the PZT Nb particles is around  $-35 \text{ mV}$ . The zeta potential and possibly the coverage of PAA on PZT Nb particles seem to be too low for an efficient dispersion of the PZT Nb particles. The presence of agglomerates and the relatively low conductivity of the suspension resulted in a nonuniform deposit. With the increasing amount of PAA to  $100 \mu\text{mol PAA/g}$ , the

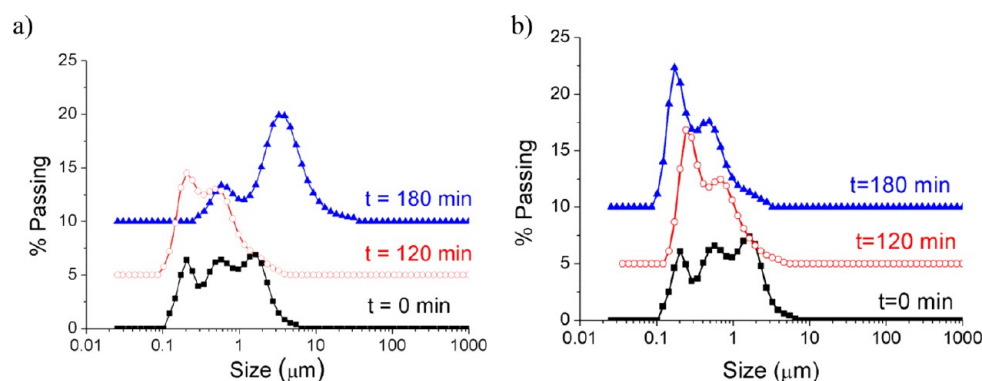


**Figure 6.** Particle-size distribution in PZT Nb suspensions milled in a colloidal mill: (a) 100 and (b) 300  $\mu\text{mol}$  PAA/g.

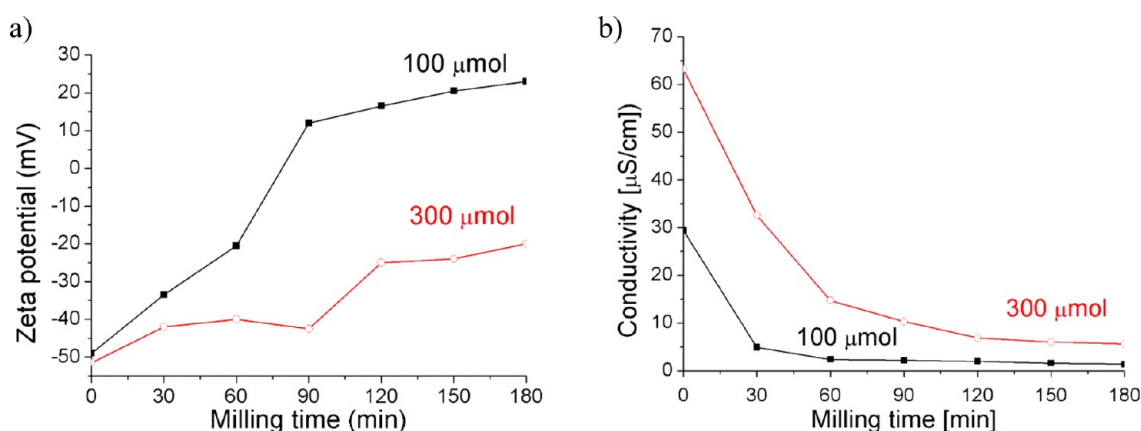


**Figure 7.** Zeta potential (a) and conductivity (b) of PZT Nb–ethanol suspensions as a function of milling time and amount of PAA: ■, 100  $\mu\text{mol}$  PAA/g; ○, 300  $\mu\text{mol}$  PAA/g.

conductivity and the absolute value of the zeta potential increased to 24  $\mu\text{S}/\text{cm}$  and  $-50$  mV, respectively, which both have a positive effect on the uniformity of the deposit (Figure 3). The suspension containing 150  $\mu\text{mol}$  PAA/g has the highest conductivity, i.e., 40  $\mu\text{S}/\text{cm}$ . Consequently, the mobility of the particles and the driving force for electrophoretic deposition decreases.<sup>5,25</sup> The high absolute value of the zeta potential, i.e.,  $-59$  mV, signifies that PAA interact with PZT Nb particles. The amount of PAA that we add to the suspension is relatively high, and it may be present in suspension as a free polymer. The nonadsorbing polymer in suspension may induce particle attractions and consequently the formation of agglomerates. This resulted in nonuniform deposits, which is in accordance with the literature.<sup>25</sup>

To reduce the PZT particle size, the ethanol-based suspension that contained 100  $\mu\text{mol}$  PAA/g and a PAA/BA ratio of 1:2.5 was milled in a colloidal mill. The particle-size distributions before milling and after 2 and 3 h of milling are shown in Figure 6a. Before milling, three peaks are observed at 0.2, 0.5, and 2  $\mu\text{m}$ . The mean particle size  $d_v$  was 0.77  $\mu\text{m}$ . The specific surface area of the powder measured by BET is 2.5  $\text{m}^2/\text{g}$ . We observed that the particle size decreases within the first two hours of milling. A bimodal particle size distribution was evident with peaks at 200 and 400 nm. The mean particle size  $d_v$  was 350 nm. However, with further milling, the particle size increases. The bimodal particle-size distribution peak values at 0.6 and 4  $\mu\text{m}$  indicate the agglomeration of the particles. Moreover, the sedimentation of the particles was evident within a few minutes. The suspension milled for 3 h that was allowed

to rest for 24 h showed a similar particle-size distribution to the one after 3 h of milling.

We increased the amount of PAA to 300  $\mu\text{mol}/\text{g}$  and milled the suspension under identical conditions to the previous one. The initial suspension showed an identical particle-size distribution to the one with 100  $\mu\text{mol}$  PAA/g. The bimodal particle-size distribution was evident after 2 h of milling, with peaks at 200 and 600 nm. The particle size slightly decreases after 3 h of milling. The mean particle size  $d_v$  reduced to 275 nm, and this value did not change if the suspension rested for 24 h (Figure 6 b). After the milling, the PZT Nb particles were well dispersed in the solvent, and we did not observe any sedimentation after 24 h. The specific surface area of the PZT Nb powder with 300  $\mu\text{mol}$  PAA/g milled for 3 h is 26  $\text{m}^2/\text{g}$ .

The zeta potential and the conductivity of the suspension as a function of milling time and the amount of PAA are shown in Figure 7a,b, respectively. The results showed that the zeta potential of the PZT Nb particles in the suspension containing 100  $\mu\text{mol}$  PAA/g was negative; i.e.,  $-50$  mV and  $-20$  mV after 0 and 1 h of milling, respectively. With the increasing milling time, the zeta potential reversed the sign, reaching a value of +16 mV and +23 mV after 2 and 3 h of milling, respectively. On the basis of these results, one would expect that the particles are agglomerated after 2 h of milling. However, by measuring the particle size distribution, the agglomeration was not observed before 3 h of milling (Figure 6a). It seems that 100  $\mu\text{mol}$  PAA/g PZT was sufficient to cover the entire surface of the micrometer-sized particles, i.e., particles before milling. However, the specific surface area of the particles increased

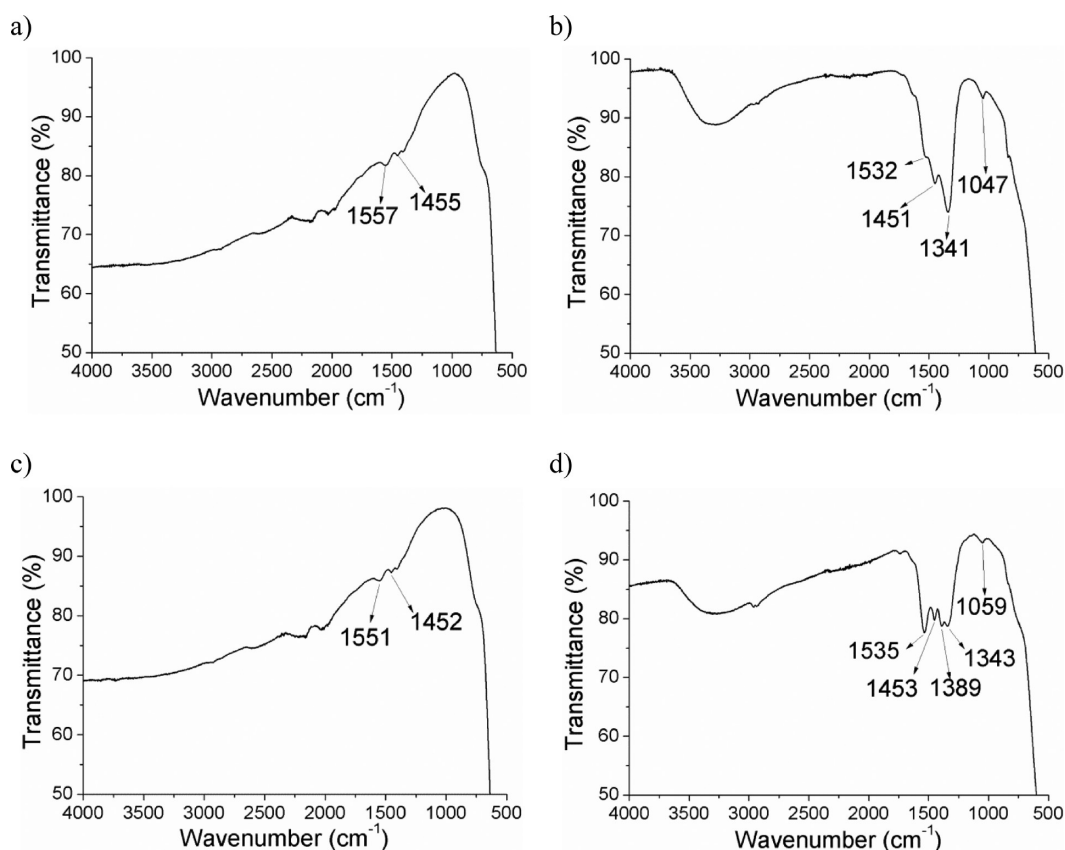


**Figure 8.** FT-IR spectra of PZT Nb powder prepared from PZT Nb suspensions with PAA/BA ratio of 1:2.5: (a) before milling, 100  $\mu\text{mol}$  PAA/g; (b) after milling, 100  $\mu\text{mol}$  PAA/g; (c) before milling, 300  $\mu\text{mol}$  PAA/g; (d) after milling, 300  $\mu\text{mol}$  PAA/g.

during the milling, and the amount of PAA was too low to cover the entire surface of the nanosized particles, and consequently, the zeta potential of the particles moved toward positive values, but the amount of PAA that was adsorbed on the particles seemed to be sufficient to keep particles separated by steric repulsion after 2 h of milling. With prolong milling time, the attraction forces prevail over the repulsive one, and the agglomeration of the particles was evident (Figure 6a). The zeta potential of the PZT Nb in the suspension containing 300  $\mu\text{mol}$  PAA/g PZT did increase from  $-50$  to a value of  $-20$  mV after 0 and 3 h of milling, respectively. In this suspension, the agglomeration was not observed (Figure 6b).

The conductivity of both suspensions decreases dramatically with the increasing milling time (Figure 7b). The conductivity of the suspension containing 300  $\mu\text{mol}$  PAA/g is higher than the conductivity of the suspension containing 100  $\mu\text{mol}$  PAA/g. The conductivities for 300 and 100  $\mu\text{mol}$  PAA/g were 65 and 30  $\mu\text{S}/\text{cm}$  before milling and 5.6 and 1.4  $\mu\text{S}/\text{cm}$ , respectively, after 3 h of milling.

From the results, it is evident that lower absolute values of the zeta potential and the conductivity were measured in the milled suspension. The specific surface area of the powder increased from 2.5 to 26  $\text{m}^2/\text{g}$  after 0 and 3 h of milling, respectively. Since the specific surface area of 3 h milled powder is approximately ten times bigger than before milling, a higher amount of PAA is needed to cover the entire PZT Nb surface. Our experiments showed that 300  $\mu\text{mol}$  PAA/g is sufficient for stabilizing fine PZT Nb particles in ethanol at these milling conditions. If there is not enough PAA, the ethanol is bonded to the particle surface, and the surface becomes positively

charged. As a result, the absolute value of the zeta potential decreases. This was observed when PZT Nb powder was milled with 100  $\mu\text{mol}$  PAA/g. The zeta potential of PZT Nb in this suspension was +20 mV; that is the value of PZT Nb in ethanol without any PAA. The conductivity of the ethanol-based suspensions is higher at higher amounts of PAA since the amount of free PAA is higher in the suspension containing 300  $\mu\text{mol}$  PAA/g than in the one with 100  $\mu\text{mol}$  PAA/g. Free PAA is dissociated in the solvent and therefore contributes to the conductivity (Figure 1b). During the milling, the specific surface area of the powder increases, PAA interacts with the new-formed surface of PZT Nb, the amount of free PAA decreases, and accordingly, the conductivity of the suspension decreased.

The interactions between PZT Nb and PAA in ethanol were studied by FT-IR (Figure 8). The FT-IR spectrum of PZT Nb/PAA shows bands in the 1600–1300  $\text{cm}^{-1}$  region and an absence of bands at 1700 and 1200  $\text{cm}^{-1}$ , similar to the PAA/BA (Figure 1). This undoubtedly suggests the anionic carboxylate form of the PAA in PZT Nb/PAA. Additionally, the significantly different shape of the 1600–1300  $\text{cm}^{-1}$  bands seen for the PAA/BA and PZT Nb/PAA FT-IR spectra indicate an electronic density shift within the carboxylate groups of the anionic PAA. The presence of the locally positively charged metal centers at the surface of the particles along to the deprotonated PAA species of the carboxylate moieties leads us to the PAA coordination onto the metal ions. This is in agreement with the zeta potential shift from positively to negatively charged particles, due to the anionic ligands



surrounding the PZT Nb particles, replacing the previous neutral ethanol molecules.

The experimental FT-IR spectra of the PZT Nb powder obtained from the suspension containing 100 and 300  $\mu\text{mol}$  PAA/g before and after the milling are shown in Figure 8. From there, it is evident that the PAA is adsorbed on the PZT Nb powder before the milling, regardless of the starting amount of PAA. An almost identical spectrum was also obtained for a 300  $\mu\text{mol}$  PAA/g PZT/PAA sample that was subject to milling for an additional 2 h. Interestingly, the IR spectrum of the PZT Nb with 100  $\mu\text{mol}$  PAA/g shows bands in the same region, but significantly reshaped, again suggesting an influence on the carboxylate bonds. This may well be related to the increased surface area of the particles as a result of the additional milling and the lower PAA concentration in the solution. There may not be enough PAA to cover all the PZT Nb surfaces, and the remaining PAA free area of PZT Nb particles may be adsorbed by the solvent ethanol. The neutral molecular ethanol thus generates the conditions of increased zeta potential (instead of anionic PAA), enabling aggregation and a simultaneously different environment for the PAA that is present. The carboxylate group with two oxygen atoms (each with two electron pairs) is highly sensitive to coordination, making several coordination modes possible.

To investigate the effect of the PVB on the properties of the suspension, we added 1 and 3 wt % of PVB to the PZT Nb suspensions that were milled for 2 h. All of the milled suspensions contained 300  $\mu\text{mol}$  PAA/g. The milled suspensions containing 0, 1, and 3 wt % of PVB are denoted as PZT Nb PVB 0, PZT Nb PVB 1, and PZT Nb PVB 3, respectively. The nonmilled PZT Nb suspension containing 100  $\mu\text{mol}$  PAA/g (denoted PZT Nb 1) is also shown. The particle size, zeta potential of PZT Nb particles, the conductivity, and the viscosity of the suspensions at  $100\text{ s}^{-1}$  are shown in Table 1. The viscosity of the suspensions as a

**Table 1. Particle Size of PZT Nb, Zeta Potential, Conductivity, and Viscosity of PZT Nb 1, PZT Nb PVB 0, PZT Nb PVB 1, and PZT Nb PVB 3 Ethanol-Based Suspensions Containing 1 Vol % of PZT Nb Powder**

	particle size $d_{v,50}$ (nm)	zeta potential (mV)	conductivity ( $\mu\text{S}/\text{cm}$ )	viscosity at $100\text{ s}^{-1}$ (mPas)
PZT Nb 1	480	−49	27	1.28
PZT Nb PVB 0	270	−27	7.7	1.53
PZT Nb PVB 1	260	−28	7.2	1.60
PZT Nb PVB 3	270	−27	10.5	1.71

function of share rate is shown in Figure 9. The viscosity of the suspensions containing 1 vol % of PZT Nb in ethanol-based solvent exhibited Newtonian-like behavior in the share rate region between 10 and  $100\text{ s}^{-1}$ , which is a reflection of the suspension stability. The lowest viscosity of 1.28 mPas was obtained for nonmilled PZT Nb suspension containing 100  $\mu\text{mol}$  PAA/g (PZT Nb 1). When we increased the amount of PAA to 300  $\mu\text{mol}$  PAA/g and reduced particle size by milling, the viscosity of the suspension increased to 1.53 mPas (suspension PZT Nb PVB 0). The addition of PVB to the milled suspension did not influence the particle size, the zeta potential of the PZT Nb, and the conductivity of this

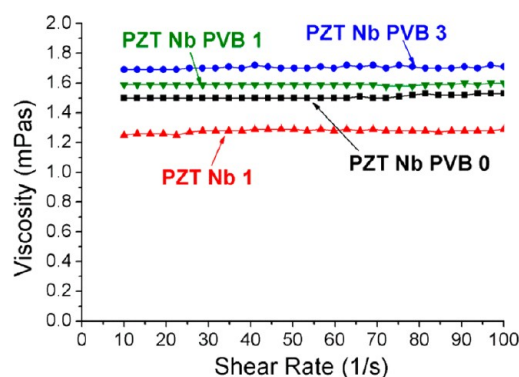


**Figure 9.** Viscosity as a function of share rate for the suspensions PZT Nb 1, PZT Nb PVB 0, PZT Nb PVB 1, and PZT Nb PVB 3.

suspension significantly. However, it increases to some extent the viscosity of the suspension from 1.53 to 1.60 and 1.71 mPas for 0, 1, and 3 wt % of PVB, respectively.

The obtained results were related to the FT-IR spectrum of the PZT Nb powder obtained from the PZT Nb PVB 3 suspension (Figure 10a). The small yield of PVB in this sample reduces, for this case, the IR method's potential since the  $1600\text{--}1300\text{ cm}^{-1}$  region is also covered by the PZT/PAA bands, the species of which are of a significantly higher yield. Nevertheless, the strongest PVB bands are in the  $1200\text{--}900\text{ cm}^{-1}$  region and, fortunately, almost free of the PZT/PAA bands. Though the bands in this region may not be as descriptive as one would wish, they clearly show almost the same features as in the IR spectrum of the free PVB (Figure 10b). Therefore, this is in agreement with the nonbonding of the PVB in this system.

The obtained IR spectra results are in accordance with previous investigations stating that PVB weakly bonds to the particle surface via hydrogen bonds that took place between the polyvinyl alcohol (PVA) functional groups and the hydroxyl groups at the particle surface.<sup>13,15</sup> However, it was reported that PVA is not bonded on  $\text{Si}_3\text{N}_4$  when the surface is modified by polymethacrylic acid.<sup>14</sup> The carboxylate group was not found to be disturbed by an OH group from the PVA.<sup>14</sup>

The electrophoretic deposition was conducted from PZT Nb 1, PZT Nb PVB 0, PZT Nb PVB 1, and PZT Nb PVB 3 suspensions. We performed the EPD experiments at a constant current density of  $1.56\text{ mA}/\text{cm}^2$  at deposition times from 15 to 150 s followed by drying the deposits in room-temperature conditions for 24 h. The masses of the deposits as a function of deposition time are shown in Figure 11.

The results indicate that the highest deposition yield was obtained from the milled suspension without a presence of PVB. The increasing amount of PVB decreased the deposition mass even though the particle size, the zeta potential of the PZT Nb, and the conductivity of the suspension did not change significantly. However, the viscosity of the suspensions slightly increased due to the presence of free PVB polymer in the suspensions. This reduced the mobility of the PZT Nb particles. The free, unadsorbed PVB chains present in the solvent established a sterical hindrance to particle movement and evidently lowered the mobility of the PZT Nb particles during EPD.

The SEM images of the as-deposited thick film from PZT Nb 1, PZT Nb PVB 0, PZT Nb PVB 1, and PZT Nb PVB 3 are shown in Figure 12a–d. The samples obtained by EPD at a constant current density of  $1.56\text{ mA}/\text{cm}^2$  for 120 s are

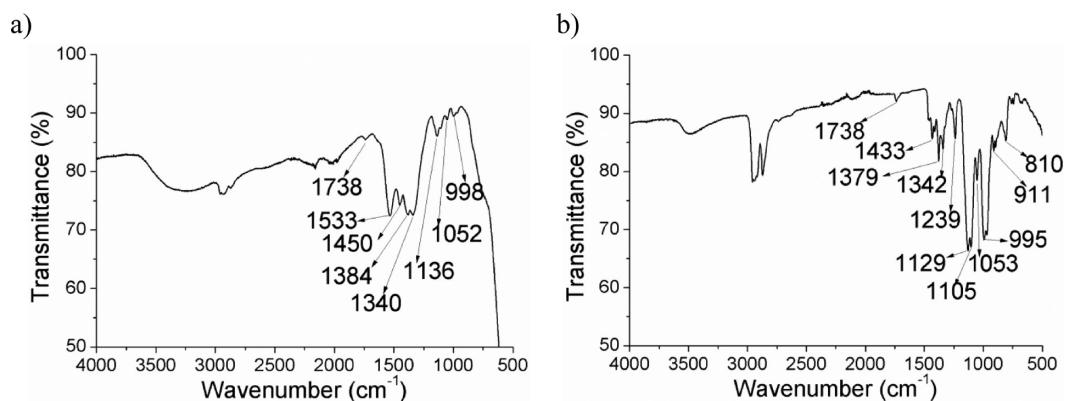


**Figure 10.** (a) FT-IR spectrum of PZT Nb powder prepared from PZT Nb PVB 3 suspension. (b) FT-IR spectrum of PVB.

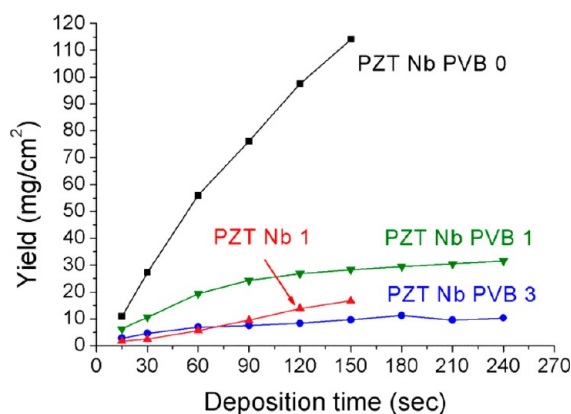


**Figure 11.** Mass of the deposit as a function of deposition time at a constant current density of  $1.56 \text{ mA/cm}^2$  obtained from the ethanol-based PZT Nb suspension with PAA/BA ratio of 1:2.5. Nonmilled PZT Nb 1 suspension contained  $100 \mu\text{mol PAA/g}$ , milled suspensions contain  $300 \mu\text{mol PAA/g}$  and 0, 1, and 3 wt % of PVB denoted as PZT Nb PVB 0, PZT Nb PVB 1, and PZT Nb PVB 3, respectively.

illustrated. The micrometer-sized PZT Nb particles are observed in the deposit from the PZT Nb 1 suspension (Figure 12a). The particles are randomly packed, resulting in a relatively porous structure. In the reported experiments, we did not observe the formation of cracks in these deposits. We think that the porous structure enables the evaporation of the solvent from the entire thickness of the deposit and that the stresses are relaxed via the pores. Moreover, the relatively low yield indicated that the thickness of the as-deposited layer is not high.

A significantly different surface morphology is obtained from the suspension PZT Nb PVB 0. The suspension was subjected to intensive milling, resulting in fine, few tens of nanometer-sized particles with high specific surface area. The mass of the deposit obtained from this suspension was six-times higher than one from PZT Nb 1 containing micrometer-sized particles, indicating the higher electrophoretic mobility of these particles. We also observed that, when the deposited mass exceeded  $100 \text{ mg/cm}^2$ , the deposits cracked after 24 h of drying. The surfaces of the PZT Nb PVB 1 and PZT Nb PVB 3 deposits were similar to the ones from PZT Nb PVB 0. The deposits obtained from the suspensions that contained PVB were smooth, and we did not observe any crack, regardless of the deposition time.

The FT-IR spectra of the deposits from the PZT Nb PVB 0 and PZT Nb PVB 3 are presented in Figure 13a,b, respectively. From the peaks around  $1550\text{--}1300 \text{ cm}^{-1}$  (the carboxylate and

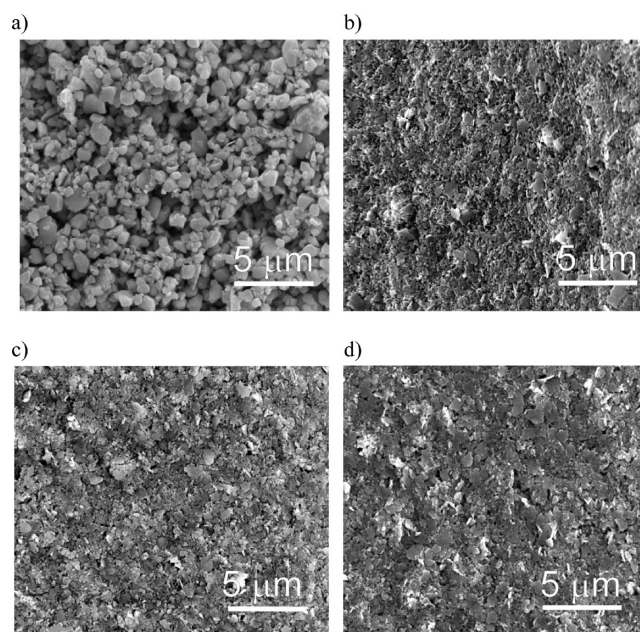


**Figure 12.** Electron microscopy surface image of as-deposited PZT Nb thick-films from ethanol suspensions. EPD was performed at a constant current density of  $1.56 \text{ mA/cm}^2$  for 120 s: (a) PZT Nb 1; (b) PZT Nb PVB 0; (c) PZT Nb PVB 1; and (d) PZT Nb PVB 3.

the C–H bonds) located at the similar positions as in the spectrum of the initial suspension (Figure 8), it is evident that the PZT Nb particles in the deposit contained PAA. We expected such results since PAA is suggested to be bonded onto the PZT Nb particles. In the FT-IR spectrum of the powder obtained from the PZT Nb PVB 3 suspension, weak intensity peaks are observed at the  $1200\text{--}900 \text{ cm}^{-1}$  region. They are characteristic for the PVB (Figure 10) whose strongest intensity signals for free PVB are present there. The obtained results demonstrated that PVB is still present in the dried deposits after the EPD is performed from a suspension containing PVB. The position and shapes of the PVB's characteristic peaks in the FT-IR spectra of the deposits and in the as-received PVB powder are very similar. From these data, we propose that there are no strong interactions between the PZT Nb–PAA and the PVB in the deposit.

## CONCLUSIONS

Piezoelectric PZT Nb thick-films were prepared from ethanol-based suspensions by electrophoretic deposition. We demon-



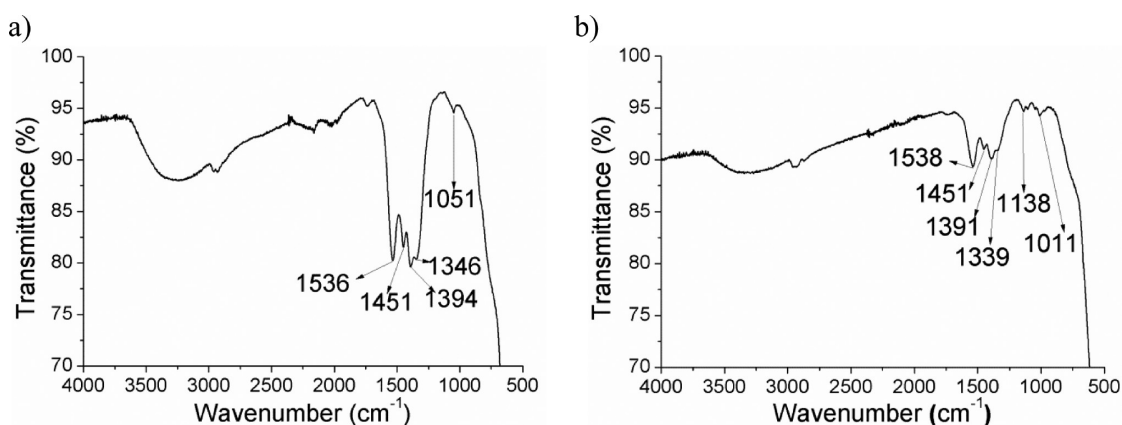


**Figure 13.** FT-IR spectra of PZT Nb deposits performed by EPD at a constant current density of 1.56 mA/cm<sup>2</sup> for 120 s. Deposits from suspension (a) PZT Nb PVB 0 and (b) PZT Nb PVB 3.

strated by Fourier-transform infrared spectroscopy that the poly(acrylic acid) is deprotonated in the presence of an organic base, butylamine, in ethanol. The deprotonated carboxyl group coordinated with the metal ions in the PZT Nb structure, which is reflected in the high absolute value of the zeta potential on the PZT Nb particles and the improved stability of the ethanol-based PZT Nb suspension. In contrast, polyvinyl butyral did not interact with the PZT Nb particles with PAA. It is present in the ethanol-based suspension as a free polymer.

The electrophoretic deposition was performed at a constant current density of 1.56 mA/cm<sup>2</sup>. The deposits obtained from the micrometer-sized PZT Nb particles stabilized with PAA exhibit a relatively porous, loosely packed structure that is not cracked. The electrophoretic yield increased when the particle size decreased to a value of a few tens of nanometers. However, the as-deposited layers cracked during drying after limiting the thickness. The deposits from PVB-containing PZT Nb suspensions are smooth and uniform. The PVB that decreased significantly the deposition yield was detected in the deposits and prevented the as-deposited layer from developing cracks.

## AUTHOR INFORMATION

### Corresponding Author

\*Tel.: 00 386 1477 3489. Fax: 00 386 1477 3887. E-mail: danjela.kuscer@ijs.si (D.K.); tina.bakaric@ijs.si (T.B.); bojan.kozlevcar@fkkt.uni-lj.si (B.K.); marija.kosec@ijs.si (M.K.).

### Notes

The authors declare no competing financial interest.

## ACKNOWLEDGMENTS

The financial support of Slovenian Research Agency is acknowledged (research programmes P2-0105 and P1-0175).

## REFERENCES

- (1) Foster, F. S.; Pavlin, C. J.; Harasiewicz, K. A.; Christopher, D. A.; Turnbull, D. H. *Ultrasound Med. Biol.* **2000**, *26*, 1–27.
- (2) Maréchal, P.; Levassort, F.; Holc, J.; Tran-Huu-Hue, L. P.; Kosec, M.; Lethiecq, M. *IEEE Trans. Ultrason. Ferroelectr. Freq. Control* **2006**, *53*, 1524–1533.
- (3) Cannata, J. M.; Ritter, T. A.; Chen, W. C.; Silverman, R. H.; Shung, K. K. *IEEE Trans. Ultrason. Ferroelectr. Freq. Control* **2003**, *50*, 1548–1557.
- (4) Kuscer, D.; Levassort, F.; Lethiecq, M.; Abellard, A.-P.; Kosec, M. *J. Am. Ceram. Soc.* **2012**, *95*, 892–900.
- (5) Ferrari, B.; Moreno, R. *J. Eur. Ceram. Soc.* **2009**, *30*, 2567–2574.
- (6) Corni, L.; Ryan, M. P.; Boccacini, A. R. *J. Eur. Ceram. Soc.* **2008**, *28*, 1353–1367.
- (7) Pedersen, H. G.; Bergstrom, L. *Acta Mater.* **2000**, *48*, 4563–4570.
- (8) Chen, H. Y. T.; Wei, W. C.; Hsu, K. C.; Chen, C. S. *J. Am. Ceram. Soc.* **2007**, *90*, 1709–1716.
- (9) Hackly, V. A. *J. Am. Ceram. Soc.* **1997**, *80*, 2315–2325.
- (10) Davies, J.; Binder, J. G. P. *J. Eur. Ceram. Soc.* **2000**, *20*, 1539–1553.
- (11) Popa, A. M.; Vleugels, J.; Vermant, J.; Van der Biest, O. *Colloids Surf., A* **2005**, *267*, 74–78.
- (12) Popa, A. M.; Vleugels, J.; Vermant, J.; Van der Biest, O. *J. Eur. Ceram. Soc.* **2006**, *16*, 933–939.
- (13) Jean, J. H.; Yeh, S.-F.; Chen, C.-J. *J. Mater. Res.* **1997**, *12*, 1062–1068.
- (14) Paik, U.; Hackley, V. A.; Lee, H.-W. *J. Am. Ceram. Soc.* **1999**, *82*, 833–8840.
- (15) Lee, J.-H.; Hyun, K.-H.; Paik, U.; Jung, Y.-G.; Lee, J.-H.; Lee, F. S.; Lee, H. S. *Colloids Surf., A* **2008**, *313–314*, 23–26.
- (16) Jason, E. G.; Scott, A. U.; Moon, J.; Cima, M. J.; Sachs, E. M. *J. Am. Ceram. Soc.* **1999**, *82*, 2080–2086.
- (17) Tang, F.; Uchikoshi, T.; Ozawa, K.; Sakka, Y. *Mater. Res. Bull.* **2002**, *37*, 653–660.
- (18) Bordia, R. K.; Raj, R. *J. Am. Ceram. Soc.* **1985**, *68*, 287–292.
- (19) Kosec, M.; Kuscer, D.; Holc, J. Processing of Ferroelectric Ceramic Thick Films. In *Multifunctional Polycrystalline Ferroelectric Materials: Processing and Properties*; Springer: New York, 2011; pp 39–41.
- (20) Wu, A.; Vilarinho, P. M.; Kingon, A. I. *J. Am. Ceram. Soc.* **2006**, *89*, 575–581.
- (21) Kang, N.; Li, J. F. *Key Eng. Mater* **2005**, *280–283*, 1899–1902.
- (22) Kaya, C.; Kaya, F.; Su, B.; Thomas, B.; Boccacini, A. R. *Surf. Coat. Technol.* **2005**, *191*, 303–310.
- (23) Damodaran, R.; Moudgil, B. M. *Colloids Surf., A* **1993**, *80*, 191–195.
- (24) Socrates, G. *Infrared Characteristic Group Frequencies*; John Wiley & Sons: New York, 1994.
- (25) Stappers, L.; Zhang, L.; Van der Biest, O.; Fransaer, J. *J. Colloid Interface Sci.* **2008**, *328*, 436–446.